Short Papers

Stability Ranges of Regenerative Frequency Dividers Employing Double Balanced Mixers in Large-Signal Operation

Rainer H. Derksen, Volker Lück, and Hans-Martin Rein

Abstract—**Regenerative frequency dividers, in general, may suffer from frequency ranges of unstable operation. An analysis of the stable ranges was given by Immovilli and Mantovani in 1973. However, its usability is restricted, since small-signal operation is assumed. In recent years the first monolithically integrated regenerative frequency dividers were presented. These are examples of circuits on which the analysis of Immovilli and Mantovani is not applicable, since the quasi-small-signal assumption is not met. This paper presents a simple theory which makes it possible to calculate the frequency ranges of stable operation for a regenerative divider employing a double balanced mixer in large-signal operation. The validity of the derived formulas is tested by various network simulations. Though the presented theory is simple, it describes the boundaries of the stable ranges quite correctly.**

I. Introduction

In 1985 the first monolithic integrated regenerative frequency divider (RFD) was realized [1], [2]. The circuit concept proposed there is characterized by the use of a transimpedance stage in series with a four-quadrant multiplier as mixer [14]. Meanwhile, this circuit concept has been successfully applied to frequency dividers fabricated in different technologies [3]–[7], and even the world's fastest monolithic integrated silicon frequency divider, with a maximum input frequency of 18 GHz [5]–[7], is based on this circuit concept.

For the design of an RFD, it has to be borne in mind that an RFD may suffer from frequency ranges of instable operation [3], [8], [10]. An analysis of the stable operating ranges of an RFD has been carried out by Immovilli and Mantovani [8] (and also presented in [10]). But their theory is not applicable to any circuit concepts which do not meet the small-signal assumptions made there, for example, the kind of circuits mentioned above [1]–[7]. Therefore, a simple large-signal theory for calculating the stable ranges of this kind of RFD has been developed and will be described here.

II. Stability Conditions

The principle of operation of an RFD is quite well known and therefore is not repeated here. It was described by Miller [9] in 1939 and has also been presented in [1]–[6], [8], and [10].

Fig. 1 shows a block diagram of an RFD with the definition of the different signals. The input signal, s_i, has angular frequency

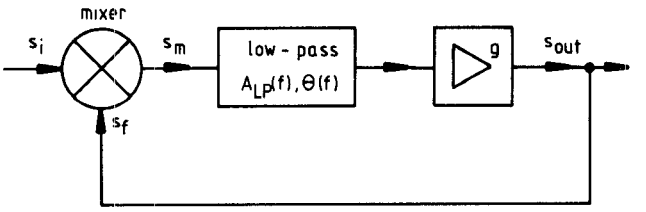

Fig. 1. Block diagram for RFD analysis.

$\omega_i (= 2\pi f_i)$, phase zero (the phase of one of the signals can be arbitrarily chosen, because only the phase relations with respect to one another are of interest), and amplitude A_i. Thus

$$s_i(t) = A_i \cos(\omega_i t). \tag{1}$$

The fed-back mixer input signal, s_f, is

$$s_f(t) = A_f \cos(\omega_i t/2 + \alpha). \tag{2}$$

It is assumed that the mixer is a double balanced one; the mixer output signal therefore has the form

$$s_m(t) = A_m \cos(\omega_i t/2 + \mu) + A_{m3} \cos(3\omega_i t/2 + \mu_3) + \cdots \tag{3}$$

and the phases $\mu, \mu_3, \mu_5, \cdots$ as well as the amplitudes $A_m, A_{m3}, A_{m5}, \cdots$ depend in general on the kind of mixer and on the mixer input quantities A_i, A_f, and α. For given A_i and A_f the remaining phase dependence $\mu = \mu(\alpha)$ will be referred to as the mixer phase characteristic.

Both the low-pass filter and the amplifier have an amplitude response and a phase response, but for the sake of simplicity the total frequency dependence is concentrated here in the low-pass filter, and the amplifier is an ideal one with gain g. Furthermore, it is assumed that only the fundamental harmonic of the signal s_m passes the low-pass filter, while all harmonics of higher order are suppressed entirely. Thus the signal s_{out} after the amplifier can be expressed as

$$s_{out}(t) = gA_{LP}A_m \cos(\omega_i t/2 + \mu + \Theta). \tag{4}$$

$A_{LP} = A_{LP}(f)$ is the magnitude and $\Theta = \Theta(f)$ the phase of the frequency response of the low-pass filter.

The signal s_{out} must be equal to the fed-back mixer input signal, s_f; thus the following amplitude condition can be obtained from (2) and (4):

$$A_f = gA_{LP}A_m \tag{5}$$

as well as the phase condition

$$\alpha = \mu + \Theta + k \cdot 2\pi, \qquad k = 0, \pm 1, \pm 2, \cdots. \tag{6}$$

Conditions (5) and (6) must be met for the steady-state operation of the divider. Attention must now be given to whether an operating point determined by (5) and (6) is stable, i.e., whether small changes of the operating point caused by disturbances decrease with time.

It is presupposed that the phase condition is independent of the amplitude condition. This restriction is required in order to

Manuscript received May 15, 1990; revised May 9, 1991.

R. H. Derksen and V. Lück were with the Institute of Electronics, Ruhr-University Bochum, D-W4630 Bochum, F. R. Germany. They are now with ANT Nachrichtentechnik GmbH, Gerberstr. 33, D-W7150 Bachnang, F. R. Germany.

H.-M. Rein is with the Institute of Electronics, Ruhr-University Bochum, D-W4630 Bochum, F. R. Germany.

IEEE Log Number 9102337.

simplify the analysis. It has subsequently been justified by testing the analytical results by network simulations.

At first, the phase condition is considered and the question whether an operating point (α_0, μ_0), with $\mu_0 = \mu(\alpha_0)$, is stable must be examined. The stability condition is calculated using the same procedure used by Immovilli and Mantovani [8]. With $\mu'(\alpha)$, the first derivative of μ with respect to α, one finds that the operating point (α_0, μ_0) is stable if

$$|\mu'(\alpha_0)| < 1. \tag{7}$$

(For the derivation, see [3].)

Taking into account that A_m is a function of A_i and A_f, the amplitude condition after (5) can be written more precisely as

$$A_f = gA_{LP}A_m(A_i, A_f). \tag{8}$$

In abbreviated form,

$$A_f = A(A_f) \tag{9}$$

is obtained for a given A_i.

Usually the function $A(x)/x$ decreases with increasing x; this is especially true for the circuits described in [1]–[7]. By virtue of this functional dependence the resulting value of A_f is both unique and stable.

III. Large-Signal Theory

A. Mixer Phase Characteristic and Stable Ranges

In this large-signal theory the simplifying approximation is made that both mixer input signals act on the mixer like a rectangular-shaped signal of large amplitude. It is presupposed here that the amplitude condition of (5) is always met and that only the signs of the signals are decisive (i.e. $s_m = +1$ if the signs of s_i and s_f are equal, and $s_m = -1$ otherwise). If, owing to small input signals, the gain inherent in the mixer becomes so small that the amplitude condition can no longer be met, the large-signal approximation is no longer permissible.

The signal after the amplifier can be written as

$$s_{out} = A_{out} \cdot \cos(\omega_i t/2 + \mu(\alpha) + \theta). \tag{10}$$

Now the mixer phase characteristic $\mu(\alpha)$ and the resulting angles Θ, α, and $\mu(\alpha)$, for which the circuit is stable, will be determined. Because of the periodicity of these quantities, it is sufficient to look at the intervals $0 \leqslant \alpha < 180°$, $0 \geqslant \mu(\alpha) > -180°$, and $0 \leqslant \Theta < 360°$.

The mixer output signal is given by

$$s_m(\omega_i t/2) = \operatorname{sign}(s_i) \cdot \operatorname{sign}(s_f) = \operatorname{sign}[\cos(\omega_i t)] \cdot \operatorname{sign}[\cos(\omega_i t/2 + \alpha)] \tag{11}$$

and its fundamental harmonic be denoted by

$$s_{m0} = A_{m0} \cdot \cos[\omega_i t/2 + \mu(\alpha)]. \tag{12}$$

By Fourier analysis of s_m (eq. (11)) the mixer phase characteristic defined by (12) can be obtained [3], [12]:

$$\mu(\alpha) = \begin{cases} 0 & \text{for } \alpha = 0 \\ \arctan[(\sqrt{2} - \cos\alpha)/\sin\alpha] - 90° & \text{for } 0 < \alpha < 45° \\ \arctan[\cos\alpha/(\sqrt{2} - \sin\alpha)] - 90° & \text{for } 45° \leqslant \alpha < 135° \\ \arctan[-(\sqrt{2} + \cos\alpha)/\sin\alpha] - 90° & \text{for } 135° \leqslant \alpha < 180° \end{cases} \tag{13}$$

From this result the stable ranges can now be determined by examining for which α the absolute value of the slope of $\mu(\alpha)$ is smaller than unity (eq. (7)). The following ranges of values for the angles α, $\mu(\alpha)$, and $\Theta = \alpha - \mu(\alpha)$ at which the circuit is stable are obtained:

$$\begin{aligned} &19° < \alpha < 71° && 109° < \alpha < 161° \\ &-35° > \mu > -55° && -125° > \mu > -145° \\ &55° < \Theta < 125° && 235° < \Theta < 305°. \end{aligned} \tag{14}$$

For the frequency ranges with stable operation, the following deductions can be made on the basis of the presented theory. The boundaries of the ranges are determined only by the total phase in the loop, without the loop gain having any influence (because the signals act like "selector switches"). Furthermore, it is true that there will be different *frequency* boundaries of the stable ranges because of different filter characteristics; however, with regard to the *total phase* Θ, the boundaries are always determined by (14). (The influence of different filter characteristics on input sensitivity versus frequency has been examined in [3].)

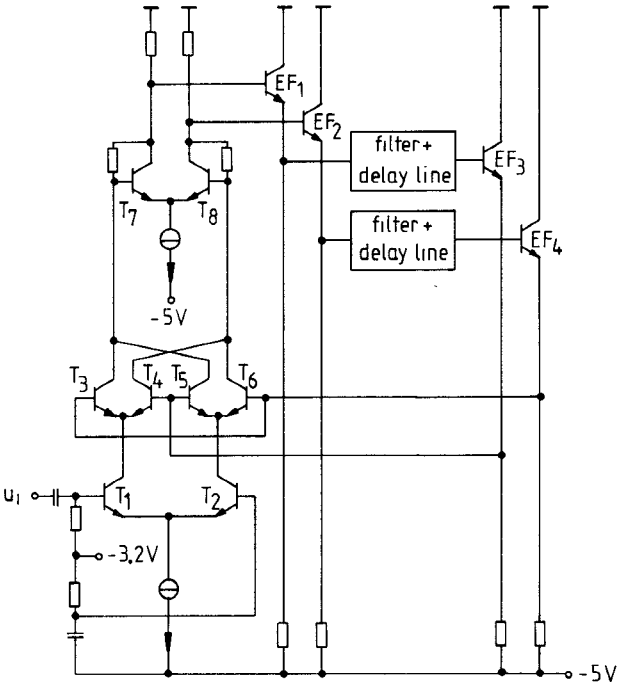

Fig. 2. Simulated circuit.

B. Test of the Validity by Simulation

A problem in the analysis of RFD's is the fact that in reality the mixer and low-pass functions are merged, in contrast to the assumption of separated nonreactive functional blocks in Fig. 1. However, to test the validity of the large-signal analysis above in subsection A, it was attempted to realize the functional blocks separately. Then the stable operating ranges of a frequency divider built up in that way were determined by simulation and compared with the calculated ones. The simulations were carried out with a special analog computer [11], which was also used for the simulation of the circuits described in [1]–[4].

The circuit in total is shown in Fig. 2, where the mixer is formed by the transistors T_1–T_8 and EF_1–EF_4. The mixer circuit (including transimpedance stage (T_7, T_8) and level shifters EF_1–EF_4) corresponds to the first stage of the 8:1 RFD described in [4], but for the simulation all the frequency-determin-

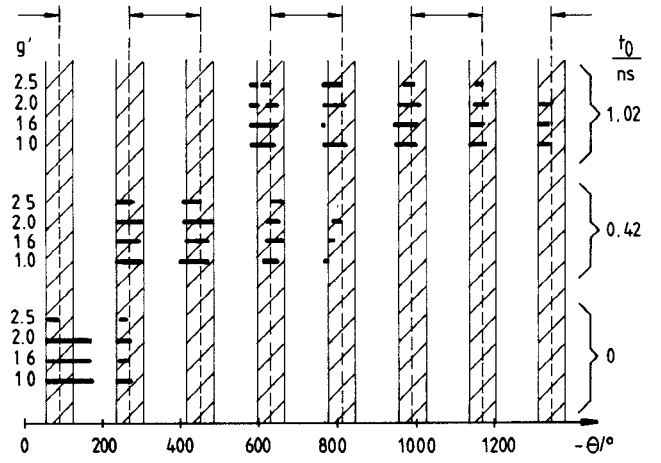

Fig. 3. Phase ranges for stable operation: comparison between simulation results (bold lines), large-signal theory presented in this work (hatched areas), and small-signal theory given in [8] (arrows).

ing transistor parasitics (junction capacitances and transit time) are set to zero. Thus, the mixer is described for all frequencies only by its dc characteristics. The frequency behavior of the loop is modeled by low-pass filters of fourth order with different amplitude and phase responses. Analog delay lines are connected in series with the filters. These lines cause a constant signal delay t_0 and a constant gain g' (both continuously adjustable). The filters are commercially available active filters. The analog delay lines are built with charge-coupled devices [12].

With this configuration, numerous simulations with different gains g' and delay times t_0 of the analog delay line as well as three different filter characteristics (Butterworth, Bessel, and *RC*) were performed [3], [12] and the frequency ranges of stable operation were identified.

From the boundaries of the frequency ranges with stable operation the total phase in the loop was determined as follows. Let f_l be the lower frequency limit of a stable range. From the phase response $\Theta_F(f)$ of the filter, the relevant phase $\Theta_{Fl} = \Theta_F(f_l/2)$ can be obtained and from the adjusted delay time t_0 the corresponding phase $\Theta_{dl} = -360° \cdot (f_l/2) \cdot t_0$ can be calculated. Thus the total phase results in

$$\Theta_l = \Theta_{Fl} - 180° \cdot f_l \cdot t_0. \tag{15}$$

Analogously, the following equation is obtained for the phase Θ_u belonging to the upper frequency limit, f_u, of a stable range:

$$\Theta_u = \Theta_{Fu} - 180° \cdot f_u \cdot t_0. \tag{16}$$

As an example, Fig. 3 shows the phase ranges derived from the simulated frequency ranges of stable operation (f_l, f_u) by use of (15) and (16) for a Butterworth filter and for different gains g' and delay times t_0. The phase ranges, in which the circuit according to the presented large-signal theory must be stable (eq. (14)), are hatched.

Taking into account the underlying simplifications (especially the assumption of the total suppression of the harmonics in the loop signal) as well as simulation uncertainties, it can be stated that the stable ranges are quite well approximated by the theoretically calculated boundaries.

The results confirm the decisive influence of the total phase being effective in the loop. If the change of the phase with frequency or the loop delay is large, the usable (stable) frequency band splits into several narrow frequency bands. In consequence, for the design of a divider, which is to have a maximum divider frequency as high as possible and an unsplit usable frequency band as large as possible, two limitations have to be taken into account. One of these is the cutoff frequency, where the loop gain falls below unity; the other is that the phase Θ changes with frequency as little as possible and only within the boundaries given by (14).

In contrast to the theory presented here, a trial application of the formulas derived in [8] to large-signal operation gives rather poor results. (It should be noted once more that the derivation in [8] is based on small-signal analysis.) This is demonstrated in Fig. 3, where one of two possible sets of stable ranges according to [8] are indicated by arrows. (For the other set the stable ranges of the first set are unstable and vice versa, the boundaries of the ranges remaining unchanged. In any event the result of the comparison would be the same.) The boundaries of the stable ranges according to [8] are exactly in the middle of the stable ranges calculated from the presented large-signal theory. This means in particular that an actually unstable range lies within a range which will be stable according to [8]. In consequence, the formulas given in [8] cannot be applied to the kind of frequency dividers investigated in this work.

IV. Final Remarks

The large-signal theory presented here has been developed because the available analysis by Immovilli and Mantovani is not applicable to the important circuit concept used in [1]–[7] for monolithic integrated high-speed frequency dividers. But, of course, it is of more general benefit for RFD's and also has been successfully used to analyze RFD's built of discrete GaAs dual-gate MESFET's [13].

It has been found that, in spite of the relatively simple assumptions for the description of the large-signal behavior, the boundaries of the stable ranges are described with sufficient accuracy by the derived analytical relations.

References

[1] R. H. Derksen, H.-M. Rein, and K. Wörner, "A monolithic 5 GHz frequency divider IC fabricated with a standard bipolar technology," in *ESSCIRC '85 Tech. Dig.* (Toulouse, France), Sept. 1985, pp. 396–400.

[2] R. H. Derksen, H.-M. Rein, and K. Wörner, "Monolithic integration of a 5.3 GHz regenerative frequency divider using a standard bipolar technology," *Electron. Lett.*, vol. 21, pp. 1037–1039, Oct. 1985.

[3] R. H. Derksen, "Monolithisch integrierte regenerative Frequenzteiler in Silizium-Bipolartechnologie für den GHz-Bereich und ihr Vergleich mit anderen Teilerprinzipien," Dr.-Ing. thesis, Ruhr-University Bochum, Bochum, F. R. Germany, 1987.

[4] R. H. Derksen and H.-M. Rein, "7.3-GHz dynamic frequency dividers monolithically integrated in a standard bipolar technology," *IEEE Trans. Microwave Theory Tech.*, vol. 36, pp. 537–541, Mar. 1988.

[5] H. Ichino *et al.*, "Super-self aligned process technology (SST) and its applications," in *Proc. IEEE 1988 Bipolar Circuits & Technology Meeting* (Minneapolis), Sept. 1988, pp. 15–18.

[6] H. Ichino *et al.*, "18-GHz 1/8 dynamic frequency divider using Si bipolar technologies," *IEEE J. Solid-State Circuits*, vol. 24, pp. 1723–1728, Dec. 1989.

[7] R. H. Derksen, "Comment on '18-GHz 1/8 dynamic frequency divider using Si bipolar technologies'," *IEEE J. Solid-State Circuits*, vol. 26, Aug. 1991.

[8] G. Immovilli and G. Mantovani, "Analysis of the Miller frequency divider by two in view of applications to wideband FM signals," *Alta Frequenza*, vol. XLII, pp. 313E(584)–323(593), Nov. 1973.

[9] R. L. Miller, "Fractional-frequency generators utilizing regenerative modulation," *Proc. IRE*, vol. 27, pp. 446–457, July 1939.

[10] R. G. Harrison, "Theory of regenerative frequency dividers using double-balanced mixers," in *1989 IEEE MTT-S. Int. Microwave Symp. Dig.*, pp. 459–462.
[11] R. Ranfft and H.-M. Rein, "A simple but efficient analog computer for simulation of high-speed integrated circuits," *IEEE J. Solid-State Circuits*, vol. SC-12, pp. 51–58, Feb. 1977.
[12] V. Lück, "Untersuchungen an einem regenerativen Frequenzteiler für den GHz-Bereich," Diploma thesis, Inst. of Electronics of Ruhr-University Bochum, Arbeitsgruppe Halbleiterbauelemente, Bochum, F. R. Germany, 1985.
[13] G. Hüther, "Dynamische Teiler für Anwendungen in der digitalen Gigabit/s-Technik," Diploma thesis, Inst. of Technical Electronics of the Technical University of Aachen, Aachen, F. R. Germany, 1988.
[14] H.-M. Rein, "Dynamischer Frequenzteiler mit Mischstufe und Verstärker," G. German patent P 3509 327, 1987.

A Multistrip Moment Method Technique and Its Application to the Post Problem in a Circular Waveguide

Xiao-Hui Zhu, Dai-Zong Chen, and Shi-Jin Wang

Abstract—**A moment method technique for solving obstacle problems in a waveguide is presented. Instead of the procedure using a multifilament current representation, which leads to a slowly converging series, a multistrip representation of the current is proposed. In the procedure, the true currents on obstacle surfaces are replaced by equivalent planar currents in a number of waveguide cross sections inside the obstacle. The technique is applied to a pair of metallic posts in the TE_{11}-mode circular waveguide. Numerical results are compared with experimental data.**

I. Introduction

The moment method (MM) is one of the most efficient numerical methods and has been widely used for solving such waveguide problems as discontinuities, junctions, transitions, excitations, obstacles, and eigenvalue problems [1]–[9]. For the inductive post in a rectangular waveguide, a two-dimensional MM solution was developed by Leviatan *et al.* [5], [6], who computed the parameters of the equivalent circuit and current distribution for a post of large diameter. For the probe-excited rectangular waveguide, a three-dimensional MM solution was developed by Jarem [7], who gave the input impedance and surface currents on the probe. These MM solutions used a multifilament current representation for the post, or probe; we refer to these as multifilament MM's. In the multifilament MM procedure, the true electric currents induced on the obstacle surfaces are replaced by a number of filamentary currents inside the obstacles. The boundary condition is then tested on the obstacle surfaces and a set of linear equations, i.e., a matrix equation, is derived. A shortcoming of the multifilament MM is that the value of matrix elements tends to infinity as the electric-field testing point approaches the filament. If the Green's function is expressed as an infinite summation of normal mode functions which satisfy the boundary condition on the waveguide wall, the matrix elements will be led to a slowly converging series, which is not convenient for computation. In a rectangular waveguide, fortunately, this series can be converted to a rapidly converging one by introducing an auxiliary series [5]–[7], or the static Green's function [2], and the multifilament MM can then be used successfully for the post and probe problems. In waveguides having other cross sections, to the authors' knowledge, such an auxiliary series is difficult to find. As a result, the multifilament MM has only a restricted application.

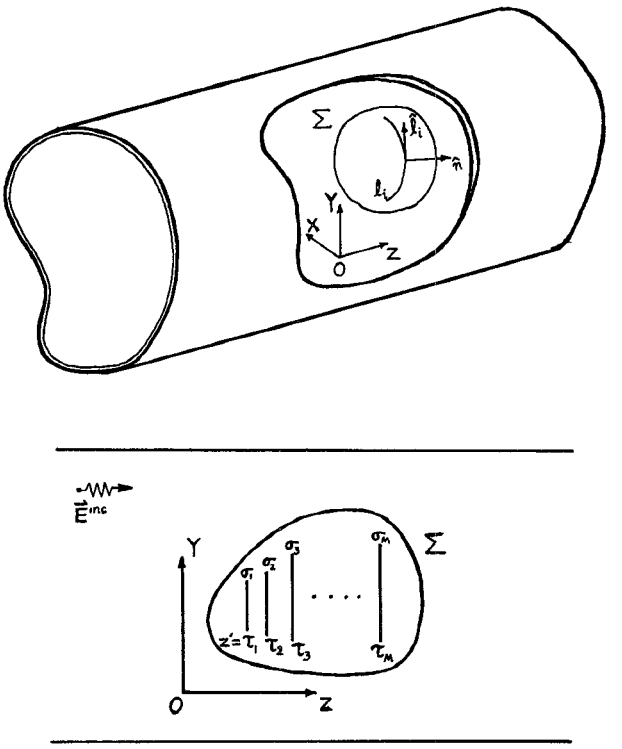

Fig. 1. Obstacle and imaginary strips in a waveguide.

In this paper, a multistrip current representation is introduced to develop a moment method technique for obstacle problems in waveguides of arbitrary section. The true currents on the obstacle surfaces are replaced by equivalent planar currents in a number of waveguide cross sections inside the obstacle, and the unknown planar currents are then expanded. The matrix equation is obtained by testing the tangential electric fields along properly chosen matching lines on the obstacle surfaces. The multistrip MM procedure will be described formally in Section II.

In a circular waveguide, the concentric discontinuities have been studied by many authors [8], [9]. By contrast, there has been little study of nonaxisymmetric discontinuities of circular waveguides, especially those with finite thickness. The multistrip MM should prove useful in solving such problems. The case of a pair of posts in a TE_{11}-mode circular waveguide will be analyzed in Section III.

II. Basic Formulation

The problem considered is depicted in Fig. 1. An obstacle is located in a cylindrical waveguide of arbitrary cross section whose axis is in the z direction. Extending the procedure to a

Manuscript received September 13, 1990; revised May 2, 1991.
The authors are with the Beijing Institute of Radio Measurement, Beijing 100039, People's Republic of China.
IEEE Log Number 9102329.